

PowerGraph: Distributed Graph-Parallel Computation on Natural Graphs

Joseph E. Gonzalez
Carnegie Mellon University
jegonzal@cs.cmu.edu

Yucheng Low
Carnegie Mellon University
ylow@cs.cmu.edu

Haijie Gu
Carnegie Mellon University
haijieg@cs.cmu.edu

Danny Bickson
Carnegie Mellon University
bickson@cs.cmu.edu

Carlos Guestrin
University of Washington
guestrin@cs.washington.edu

Abstract

Large-scale graph-structured computation is central to tasks ranging from targeted advertising to natural language processing and has led to the development of several graph-parallel abstractions including Pregel and GraphLab. However, the natural graphs commonly found in the real-world have highly skewed power-law degree distributions, which challenge the assumptions made by these abstractions, limiting performance and scalability.

In this paper, we characterize the challenges of computation on natural graphs in the context of existing graph-parallel abstractions. We then introduce the PowerGraph abstraction which exploits the internal structure of graph programs to address these challenges. Leveraging the PowerGraph abstraction we introduce a new approach to distributed graph placement and representation that exploits the structure of power-law graphs. We provide a detailed analysis and experimental evaluation comparing PowerGraph to two popular graph-parallel systems. Finally, we describe three different implementation strategies for PowerGraph and discuss their relative merits with empirical evaluations on large-scale real-world problems demonstrating order of magnitude gains.

1 Introduction

The increasing need to reason about large-scale graph-structured data in machine learning and data mining (MLDM) presents a critical challenge. As the sizes of datasets grow, statistical theory suggests that we should apply richer models to eliminate the unwanted bias of simpler models, and extract stronger signals from data. At the same time, the computational and storage complexity of richer models coupled with rapidly growing datasets have exhausted the limits of single machine computation.

The resulting demand has driven the development of new *graph-parallel* abstractions such as Pregel [30] and GraphLab [29] that encode computation as *vertex-programs* which run in parallel and interact along edges

in the graph. Graph-parallel abstractions rely on each vertex having a small neighborhood to maximize parallelism and effective partitioning to minimize communication. However, graphs derived from real-world phenomena, like social networks and the web, typically have *power-law* degree distributions, which implies that a small subset of the vertices connects to a large fraction of the graph. Furthermore, power-law graphs are difficult to partition [1, 28] and represent in a distributed environment.

To address the challenges of power-law graph computation, we introduce the PowerGraph abstraction which exploits the structure of vertex-programs and explicitly factors computation over edges instead of vertices. As a consequence, PowerGraph exposes substantially greater parallelism, reduces network communication and storage costs, and provides a new highly effective approach to distributed graph placement. We describe the design of our distributed implementation of PowerGraph and evaluate it on a large EC2 deployment using real-world applications. In particular our key contributions are:

1. An analysis of the challenges of power-law graphs in distributed graph computation and the limitations of existing graph parallel abstractions (Sec. 2 and 3).
2. The PowerGraph abstraction (Sec. 4) which factors individual vertex-programs.
3. A delta caching procedure which allows computation state to be dynamically maintained (Sec. 4.2).
4. A new fast approach to data layout for power-law graphs in distributed environments (Sec. 5).
5. An theoretical characterization of network and storage (Theorem 5.2, Theorem 5.3).
6. A high-performance open-source implementation of the PowerGraph abstraction (Sec. 7).
7. A comprehensive evaluation of three implementations of PowerGraph on a large EC2 deployment using real-world MLDM applications (Sec. 6 and 7).

2 Graph-Parallel Abstractions

A **graph-parallel** abstraction consists of a *sparse* graph $G = \{V, E\}$ and a **vertex-program** Q which is executed in parallel on each vertex $v \in V$ and can interact (e.g., through shared-state in GraphLab, or messages in Pregel) with neighboring instances $Q(u)$ where $(u, v) \in E$. In contrast to more general message passing models, graph-parallel abstractions constrain the interaction of vertex-program to a graph structure enabling the optimization of data-layout and communication. We focus our discussion on Pregel and GraphLab as they are representative of existing graph-parallel abstractions.

2.1 Pregel

Pregel [30] is a bulk synchronous *message passing* abstraction in which all vertex-programs run simultaneously in a sequence of super-steps. Within a **super-step** each program instance $Q(v)$ receives all messages from the previous super-step and sends messages to its neighbors in the next super-step. A barrier is imposed between super-steps to ensure that all program instances finish processing messages from the previous super-step before proceeding to the next. The program terminates when there are no messages remaining and every program has voted to halt. Pregel introduces commutative associative message **combiners** which are user defined functions that merge messages destined to the same vertex. The following is an example of the PageRank vertex-program implemented in Pregel. The vertex-program receives the single incoming message (after the combiner) which contains the sum of the PageRanks of all in-neighbors. The new PageRank is then computed and sent to its out-neighbors.

```
Message combiner(Message m1, Message m2) :
    return Message(m1.value() + m2.value());
void PregelPageRank(Message msg) :
    float total = msg.value();
    vertex.val = 0.15 + 0.85*total;
    foreach(nbr in out_neighbors) :
        SendMsg(nbr, vertex.val/num_out_nbrs);
```

2.2 GraphLab

GraphLab [29] is an *asynchronous distributed shared-memory* abstraction in which vertex-programs have shared access to a distributed graph with data stored on every vertex and edge. Each vertex-program may directly access information on the current vertex, adjacent edges, and adjacent vertices irrespective of edge direction. Vertex-programs can schedule neighboring vertex-programs to be executed in the future. GraphLab ensures serializability by preventing neighboring program instances from running simultaneously. The following is an example of the PageRank vertex-program implemented in GraphLab. The GraphLab vertex-program directly reads neighboring vertex values to compute the sum.

```
void GraphLabPageRank(Scope scope) :
    float accum = 0;
    foreach (nbr in scope.in_nbrs) :
        accum += nbr.val / nbr.nout_nbrs();
    vertex.val = 0.15 + 0.85 * accum;
```

By eliminating messages, GraphLab isolates the user defined algorithm from the movement of data, allowing the system to choose when and how to move program state. By allowing mutable data to be associated with both vertices *and edges* GraphLab allows the algorithm designer to more precisely distinguish between data shared with all neighbors (vertex data) and data shared with a particular neighbor (edge data).

2.3 Characterization

While the implementation of MLDM vertex-programs in GraphLab and Pregel differ in how they collect and disseminate information, they share a common overall structure. To characterize this common structure and differentiate between vertex and edge specific computation we introduce the GAS model of graph computation.

The **GAS** model represents three *conceptual* phases of a vertex-program: **Gather**, **Apply**, and **Scatter**. In the **gather** phase, information about adjacent vertices and edges is collected through a generalized sum over the neighborhood of the vertex u on which $Q(u)$ is run:

$$\Sigma \leftarrow \bigoplus_{v \in \mathbf{Nbr}[u]} g(D_u, D_{(u,v)}, D_v). \quad (2.1)$$

where D_u , D_v , and $D_{(u,v)}$ are the values (program state and meta-data) for vertices u and v and edge (u, v) . The user defined sum \oplus operation must be commutative and associative and can range from a numerical sum to the union of the data on all neighboring vertices and edges.

The resulting value Σ is used in the **apply** phase to update the value of the central vertex:

$$D_u^{\text{new}} \leftarrow a(D_u, \Sigma). \quad (2.2)$$

Finally the **scatter** phase uses the new value of the central vertex to update the data on adjacent edges:

$$\forall v \in \mathbf{Nbr}[u] : \left(D_{(u,v)} \right) \leftarrow s \left(D_u^{\text{new}}, D_{(u,v)}, D_v \right). \quad (2.3)$$

The fan-in and fan-out of a vertex-program is determined by the corresponding gather and scatter phases. For instance, in PageRank, the gather phase only operates on in-edges and the scatter phase only operates on out-edges. However, for many MLDM algorithms the graph edges encode ostensibly symmetric relationships, like friendship, in which both the gather and scatter phases touch all edges. In this case the fan-in and fan-out are equal. As we will show in Sec. 3, the ability for graph parallel abstractions to support both high fan-in and fan-out computation is critical for efficient computation on natural graphs.

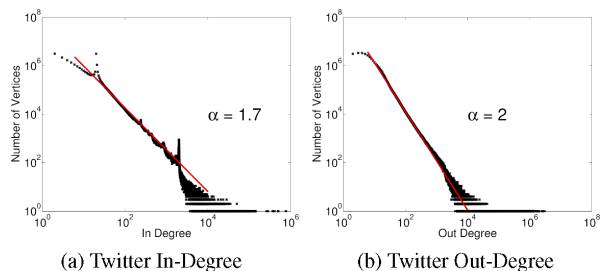


Figure 1: The in and out degree distributions of the Twitter follower network plotted in log-log scale.

GraphLab and Pregel express GAS programs in very different ways. In the Pregel abstraction the gather phase is implemented using message combiners and the apply and scatter phases are expressed in the vertex program. Conversely, GraphLab exposes the entire neighborhood to the vertex-program and allows the user to define the gather and apply phases within their program. The GraphLab abstraction implicitly defines the communication aspects of the gather/scatter phases by ensuring that changes made to the vertex or edge data are automatically visible to adjacent vertices. It is also important to note that GraphLab does not differentiate between edge directions.

3 Challenges of Natural Graphs

The sparsity structure of natural graphs presents a unique challenge to efficient distributed graph-parallel computation. One of the hallmark properties of natural graphs is their *skewed* power-law degree distribution[16]: most vertices have relatively few neighbors while a few have many neighbors (e.g., celebrities in a social network). Under a power-law degree distribution the probability that a vertex has degree d is given by:

$$P(d) \propto d^{-\alpha}, \quad (3.1)$$

where the exponent α is a positive constant that controls the “skewness” of the degree distribution. Higher α implies that the graph has lower density (ratio of edges to vertices), and that the vast majority of vertices are low degree. As α decreases, the graph density and number of high degree vertices increases. Most natural graphs typically have a power-law constant around $\alpha \approx 2$. For example, Faloutsos et al. [16] estimated that the inter-domain graph of the Internet has a power-law constant $\alpha \approx 2.2$. One can visualize the skewed power-law degree distribution by plotting the number of vertices with a given degree in log-log scale. In Fig. 1, we plot the in and out degree distributions of the Twitter follower network demonstrating the characteristic linear power-law form.

While power-law degree distributions are empirically observable, they do not fully characterize the properties of natural graphs. While there has been substantial work (see

[27]) in more sophisticated natural graph models, the techniques in this paper focus only on the degree distribution and do not require any other modeling assumptions.

The skewed degree distribution implies that a small fraction of the vertices are adjacent to a large fraction of the edges. For example, one percent of the vertices in the Twitter web-graph are adjacent to nearly half of the edges. This concentration of edges results in a *star-like* motif which presents challenges for existing graph-parallel abstractions:

Work Balance: The power-law degree distribution can lead to substantial work imbalance in graph parallel abstractions that treat vertices symmetrically. Since the storage, communication, and computation complexity of the Gather and Scatter phases is linear in the degree, the running time of vertex-programs can vary widely [36].

Partitioning: Natural graphs are difficult to partition[26, 28]. Both GraphLab and Pregel depend on graph partitioning to minimize communication and ensure work balance. However, in the case of natural graphs both are forced to resort to hash-based (random) partitioning which has extremely poor locality (Sec. 5).

Communication: The skewed degree distribution of natural-graphs leads to communication asymmetry and consequently bottlenecks. In addition, high-degree vertices can force messaging abstractions, such as Pregel, to generate and send many identical messages.

Storage: Since graph parallel abstractions must locally store the adjacency information for each vertex, each vertex requires memory linear in its degree. Consequently, high-degree vertices can exceed the memory capacity of a single machine.

Computation: While multiple vertex-programs may execute in parallel, existing graph-parallel abstractions do not parallelize *within* individual vertex-programs, limiting their scalability on high-degree vertices.

4 PowerGraph Abstraction

To address the challenges of computation on power-law graphs, we introduce PowerGraph, a new graph-parallel abstraction that eliminates the degree dependence of the vertex-program by directly exploiting the GAS decomposition to factor vertex-programs over edges. By lifting the Gather and Scatter phases into the abstraction, PowerGraph is able to retain the natural “think-like-a-vertex” philosophy [30] while distributing the computation of a single vertex-program over the entire cluster.

PowerGraph combines the best features from both Pregel and GraphLab. From GraphLab, PowerGraph borrows the data-graph and shared-memory view of computation eliminating the need for users to architect the movement of information. From Pregel, PowerGraph borrows the commutative, associative gather concept. PowerGraph

```

interface GASVertexProgram(u) {
  // Run on gather_nbrs(u)
  gather( $D_u, D_{(u,v)}, D_v$ )  $\rightarrow$  Accum
  sum(Accum left, Accum right)  $\rightarrow$  Accum
  apply( $D_u, Accum$ )  $\rightarrow$   $D_u^{new}$ 
  // Run on scatter_nbrs(u)
  scatter( $D_u^{new}, D_{(u,v)}, D_v$ )  $\rightarrow$  ( $D_{(u,v)}^{new}, Accum$ )
}

```

Figure 2: All PowerGraph programs must implement the stateless gather, sum, apply, and scatter functions.

Algorithm 1: Vertex-Program Execution Semantics

Input: Center vertex u

if cached accumulator a_u is empty **then**

foreach neighbor v in $gather_nbrs(u)$ **do**

$a_u \leftarrow sum(a_u, gather(D_u, D_{(u,v)}, D_v))$

end

end

$D_u \leftarrow apply(D_u, a_u)$

foreach neighbor v in $scatter_nbrs(u)$ **do**

$(D_{(u,v)}, \Delta a) \leftarrow scatter(D_u, D_{(u,v)}, D_v)$

if a_v and Δa are not Empty **then** $a_v \leftarrow sum(a_v, \Delta a)$

else $a_v \leftarrow Empty$

end

supports both the highly-parallel bulk-synchronous Pregel model of computation as well as the computationally efficient asynchronous GraphLab model of computation.

Like GraphLab, the state of a PowerGraph program factors according to a **data-graph** with user defined vertex data D_v and edge data $D_{(u,v)}$. The data stored in the data-graph includes both meta-data (e.g., urls and edge weights) as well as computation state (e.g., the PageRank of vertices). In Sec. 5 we introduce vertex-cuts which allow PowerGraph to efficiently represent and store power-law graphs in a distributed environment. We now describe the PowerGraph *abstraction* and how it can be used to naturally decompose vertex-programs. Then in Sec. 5 through Sec. 7 we discuss how to implement the PowerGraph abstraction in a distributed environment.

4.1 GAS Vertex-Programs

Computation in the PowerGraph abstraction is encoded as a stateless **vertex-program** which implements the GASVertexProgram interface (Fig. 2) and therefore explicitly factors into the gather, sum, apply, and scatter functions. Each function is invoked in stages by the PowerGraph engine following the semantics in Alg. 1. By factoring the vertex-program, the PowerGraph execution engine can distribute a single vertex-program over multiple machines and move computation to the data.

During the gather phase the `gather` and `sum` functions are used as a *map* and *reduce* to collect information

about the neighborhood of the vertex. The `gather` function is invoked in parallel on the edges adjacent to u . The particular set of edges is determined by `gather_nbrs` which can be `none`, `in`, `out`, or `all`. The `gather` function is passed the data on the adjacent vertex and edge and returns a temporary accumulator (a user defined type). The result is combined using the commutative and associative `sum` operation. The final result a_u of the gather phase is passed to the `apply` phase and cached by PowerGraph.

After the gather phase has completed, the `apply` function takes the final accumulator and computes a new vertex value D_u which is atomically written back to the graph. The size of the accumulator a_u and complexity of the `apply` function play a central role in determining the network and storage efficiency of the PowerGraph abstraction and should be *sub-linear* and ideally constant in the degree.

During the scatter phase, the `scatter` function is invoked in parallel on the edges adjacent to u producing new edge values $D_{(u,v)}$ which are written back to the data-graph. As with the gather phase, the `scatter_nbrs` determines the particular set of edges on which scatter is invoked. The scatter function returns an optional value Δa which is used to dynamically update the cached accumulator a_v for the adjacent vertex (see Sec. 4.2).

In Fig. 3 we implement the PageRank, greedy graph coloring, and single source shortest path algorithms using the PowerGraph abstraction. In PageRank the gather and sum functions collect the total value of the adjacent vertices, the apply function computes the new PageRank, and the scatter function is used to activate adjacent vertex-programs if necessary. In graph coloring the gather and sum functions collect the set of colors on adjacent vertices, the apply function computes a new color, and the scatter function activates adjacent vertices if they violate the coloring constraint. Finally in single source shortest path (SSSP), the gather and sum functions compute the shortest path through each of the neighbors, the apply function returns the new distance, and the scatter function activates affected neighbors.

4.2 Delta Caching

In many cases a vertex-program will be triggered in response to a change in a *few* of its neighbors. The gather operation is then repeatedly invoked on *all* neighbors, many of which remain unchanged, thereby wasting computation cycles. For many algorithms [2] it is possible to dynamically maintain the result of the gather phase a_u and skip the gather on subsequent iterations.

The PowerGraph engine maintains a cache of the accumulator a_u from the previous gather phase for each vertex. The scatter function can *optionally* return an additional Δa which is atomically added to the cached accumulator a_v of the neighboring vertex v using the `sum` function. If Δa is not returned, then the neighbor's cached a_v is cleared,

PageRank

```

// gather_nbrs: IN_NBRs
gather(Du, D(u,v), Dv):
    return Dv.rank / #outNbrs(v)
sum(a, b): return a + b
apply(Du, acc):
    rnew = 0.15 + 0.85 * acc
    Du.delta = (rnew - Du.rank) /
                #outNbrs(u)
    Du.rank = rnew
// scatter_nbrs: OUT_NBRs
scatter(Du, D(u,v), Dv):
    if(|Du.delta| > ε) Activate(v)
    return delta

```

Greedy Graph Coloring

```

// gather_nbrs: ALL_NBRs
gather(Du, D(u,v), Dv):
    return set(Dv)
sum(a, b): return union(a, b)
apply(Du, S):
    Du = min c where c ∉ S
// scatter_nbrs: ALL_NBRs
scatter(Du, D(u,v), Dv):
    // Nbr changed since gather
    if(Du == Dv)
        Activate(v)
    // Invalidate cached accum
    return NULL

```

Single Source Shortest Path (SSSP)

```

// gather_nbrs: ALL_NBRs
gather(Du, D(u,v), Dv):
    return Dv + D(v,u)
sum(a, b): return min(a, b)
apply(Du, new_dist):
    Du = new_dist
// scatter_nbrs: ALL_NBRs
scatter(Du, D(u,v), Dv):
    // If changed activate neighbor
    if(changed(Du)) Activate(v)
    if(increased(Du))
        return NULL
    else return Du + D(u,v)

```

Figure 3: The PageRank, graph-coloring, and single source shortest path algorithms implemented in the PowerGraph abstraction. Both the PageRank and single source shortest path algorithms support delta caching in the gather phase.

forcing a complete gather on the subsequent execution of the vertex-program on the vertex v . When executing the vertex-program on v the PowerGraph engine uses the cached a_v if available, bypassing the gather phase.

Intuitively, Δa acts as an additive correction on-top of the previous gather for that edge. More formally, if the accumulator type forms an **abelian group**: has a commutative and associative sum (+) and an *inverse* (−) operation, then we can define (shortening `gather` to g):

$$\Delta a = g(D_u, D_{(u,v)}^{\text{new}}, D_v^{\text{new}}) - g(D_u, D_{(u,v)}, D_v). \quad (4.1)$$

In the PageRank example (Fig. 3) we take advantage of the abelian nature of the PageRank sum operation. For graph coloring the set union operation is not abelian and so we invalidate the accumulator.

4.3 Initiating Future Computation

The PowerGraph engine maintains a set of active vertices on which to eventually execute the vertex-program. The user initiates computation by calling `Activate(v)` or `Activate_all()`. The PowerGraph engine then proceeds to execute the vertex-program on the active vertices until none remain. Once a vertex-program completes the scatter phase it becomes inactive until it is reactivated.

Vertices can activate themselves and neighboring vertices. Each function in a vertex-program can only activate vertices visible in the arguments to that function. For example the scatter function invoked on the edge (u, v) can only activate the vertices u and v . This restriction is essential to ensure that activation events are generated on machines on which they can be efficiently processed.

The order in which activated vertices are executed is up to the PowerGraph execution engine. The only guarantee is that all activated vertices are eventually executed. This flexibility in scheduling enables PowerGraph programs to be executed both *synchronously* and *asynchronously*, leading to different tradeoffs in algorithm performance, system performance, and determinism.

4.3.1 Bulk Synchronous Execution

When run synchronously, the PowerGraph engine executes the gather, apply, and scatter phases in order. Each phase, called a **minor-step**, is run synchronously on all active vertices with a barrier at the end. We define a **super-step** as a complete series of GAS minor-steps. Changes made to the vertex data and edge data are committed at the end of each minor-step and are visible in the subsequent minor-step. Vertices activated in each super-step are executed in the subsequent super-step.

The synchronous execution model ensures a deterministic execution regardless of the number of machines and closely resembles Pregel. However, the frequent barriers and inability to operate on the most recent data can lead to an inefficient distributed execution and slow algorithm convergence. To address these limitations PowerGraph also supports asynchronous execution.

4.3.2 Asynchronous Execution

When run asynchronously, the PowerGraph engine executes active vertices as processor and network resources become available. Changes made to the vertex and edge data during the apply and scatter functions are immediately committed to the graph and visible to subsequent computation on neighboring vertices.

By using processor and network resources as they become available and making any changes to the data-graph immediately visible to future computation, an asynchronous execution can more effectively utilize resources and accelerate the convergence of the underlying algorithm. For example, the greedy graph-coloring algorithm in Fig. 3 will not converge when executed synchronously but converges quickly when executed asynchronously. The merits of asynchronous computation have been studied extensively in the context of numerical algorithms [4]. In [18, 19, 29] we demonstrated that asynchronous computation can lead to both theoretical and empirical

gains in algorithm and system performance for a range of important MLDM applications.

Unfortunately, the behavior of the asynchronous execution depends on the number machines and availability of network resources leading to non-determinism that can complicate algorithm design and debugging. Furthermore, for some algorithms, like statistical simulation, the resulting non-determinism, if not carefully controlled, can lead to instability or even divergence [17].

To address these challenges, GraphLab automatically enforces **serializability**: every parallel execution of vertex-programs has a corresponding sequential execution. In [29] it was shown that serializability is sufficient to support a wide range of MLDM algorithms. To achieve serializability, GraphLab prevents adjacent vertex-programs from running concurrently using a fine-grained locking protocol which requires *sequentially* grabbing locks on all neighboring vertices. Furthermore, the locking scheme used by GraphLab is unfair to high degree vertices.

PowerGraph retains the strong serializability guarantees of GraphLab while addressing its limitations. We address the problem of sequential locking by introducing a new *parallel* locking protocol (described in Sec. 7.4) which is fair to high degree vertices. In addition, the PowerGraph abstraction exposes substantially more fine-grained (edge-level) parallelism allowing the entire cluster to support the execution of individual vertex programs.

4.4 Comparison with GraphLab / Pregel

Surprisingly, despite the strong constraints imposed by the PowerGraph abstraction, it is *possible* to emulate both GraphLab and Pregel vertex-programs in PowerGraph. To emulate a GraphLab vertex-program, we use the gather and sum functions to *concatenate* all the data on adjacent vertices and edges and then run the GraphLab program within the apply function. Similarly, to express a Pregel vertex-program, we use the gather and sum functions to combine the inbound messages (stored as edge data) and *concatenate* the list of neighbors needed to compute the outbound messages. The Pregel vertex-program then runs within the apply function generating the set of messages which are passed as vertex data to the scatter function where they are written back to the edges.

In order to address the challenges of natural graphs, the PowerGraph abstraction requires the size of the accumulator and the complexity of the apply function to be sub-linear in the degree. However, directly executing GraphLab and Pregel vertex-programs within the apply function leads the size of the accumulator and the complexity of the apply function to be *linear* in the degree eliminating many of the benefits on natural graphs.

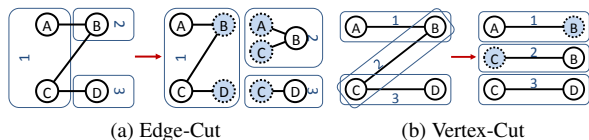


Figure 4: (a) An edge-cut and (b) vertex-cut of a graph into three parts. Shaded vertices are ghosts and mirrors respectively.

5 Distributed Graph Placement

The PowerGraph abstraction relies on the distributed data-graph to store the computation state and encode the interaction between vertex-programs. The placement of the data-graph structure and data plays a central role in minimizing communication and ensuring work balance.

A common approach to placing a graph on a cluster of p machines is to construct a balanced p -way **edge-cut** (e.g., Fig. 4a) in which vertices are evenly assigned to machines and the number of edges spanning machines is minimized. Unfortunately, the tools [23, 31] for constructing balanced edge-cuts perform poorly [1, 28, 26] on power-law graphs. When the graph is difficult to partition, both GraphLab and Pregel resort to hashed (random) vertex placement. While fast and easy to implement, hashed vertex placement cuts most of the edges:

Theorem 5.1. *If vertices are randomly assigned to p machines then the expected fraction of edges cut is:*

$$\mathbb{E} \left[\frac{|\text{Edges Cut}|}{|E|} \right] = 1 - \frac{1}{p}. \quad (5.1)$$

For a power-law graph with exponent α , the expected number of edges cut per-vertex is:

$$\mathbb{E} \left[\frac{|\text{Edges Cut}|}{|V|} \right] = \left(1 - \frac{1}{p} \right) \mathbb{E} [\mathbf{D}[v]] = \left(1 - \frac{1}{p} \right) \frac{\mathbf{h}_{|V|}(\alpha - 1)}{\mathbf{h}_{|V|}(\alpha)}, \quad (5.2)$$

where the $\mathbf{h}_{|V|}(\alpha) = \sum_{d=1}^{|V|-1} d^{-\alpha}$ is the normalizing constant of the power-law Zipf distribution.

Proof. An edge is cut if both vertices are randomly assigned to different machines. The probability that both vertices are assigned to different machines is $1 - 1/p$. \square

Every cut edge contributes to storage and network overhead since both machines maintain a copy of the adjacency information and in some cases [20], a **ghost** (local copy) of the vertex and edge data. For example in Fig. 4a we construct a three-way edge-cut of a four vertex graph resulting in five ghost vertices and all edge data being replicated. Any changes to vertex and edge data associated with a cut edge must be synchronized across the network. For example, using just two machines, a random cut will cut roughly *half* the edges, requiring $|E|/2$ communication.

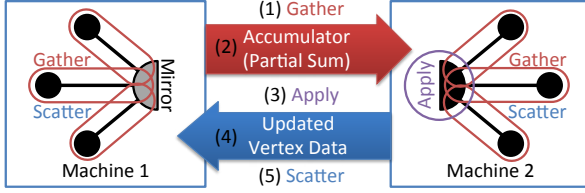


Figure 5: The communication pattern of the PowerGraph abstraction when using a vertex-cut. Gather function runs locally on each machine and then one accumulator is sent from each mirror to the master. The master runs the apply function and then sends the updated vertex data to all mirrors. Finally the scatter phase is run in parallel on mirrors.

5.1 Balanced p -way Vertex-Cut

By factoring the vertex program along the edges in the graph, The PowerGraph abstraction allows a single vertex-program to span multiple machines. In Fig. 5 a single high degree vertex program has been split across two machines with the gather and scatter functions running in parallel on each machine and accumulator and vertex data being exchanged across the network.

Because the PowerGraph abstraction allows a single vertex-program to span multiple machines, we can improve work balance and reduce communication and storage overhead by evenly *assigning edges* to machines and allowing *vertices to span machines*. Each machine only stores the edge information for the edges assigned to that machine, evenly distributing the massive amounts of edge data. Since each edge is stored exactly once, changes to edge data do not need to be communicated. However, changes to vertex must be copied to all the machines it spans, thus the storage and network overhead depend on the number of machines spanned by each vertex.

We minimize storage and network overhead by limiting the number of machines spanned by each vertex. A balanced p -way **vertex-cut** formalizes this objective by assigning each edge $e \in E$ to a machine $A(e) \in \{1, \dots, p\}$. Each vertex then spans the set of machines $A(v) \subseteq \{1, \dots, p\}$ that contain its adjacent edges. We define the balanced vertex-cut objective:

$$\min_A \frac{1}{|V|} \sum_{v \in V} |A(v)| \quad (5.3)$$

$$\text{s.t.} \quad \max_m |\{e \in E \mid A(e) = m\}|, < \lambda \frac{|E|}{p} \quad (5.4)$$

where the imbalance factor $\lambda \geq 1$ is a small constant. We use the term **replicas** of a vertex v to denote the $|A(v)|$ copies of the vertex v : each machine in $A(v)$ has a replica of v . Because changes to vertex data are communicated to all replicas, the communication overhead is also given by $|A(v)|$. The objective (Eq. 5.3) therefore minimizes the average number of replicas in the graph and as a consequence the total storage and communication requirements

of the PowerGraph engine.

For each vertex v with multiple replicas, one of the replicas is *randomly* nominated as the **master** which maintains the master version of the vertex data. All remaining replicas of v are then **mirrors** and maintain a local cached *read only* copy of the vertex data. (e.g., Fig. 4b). For instance, in Fig. 4b we construct a three-way vertex-cut of a graph yielding only 2 mirrors. Any changes to the vertex data (e.g., the Apply function) must be made to the master which is then immediately replicated to all mirrors.

Vertex-cuts address the major issues associated with edge-cuts in power-law graphs. Percolation theory [3] suggests that power-law graphs have good vertex-cuts. Intuitively, by cutting a small fraction of the very high degree vertices we can quickly shatter a graph. Furthermore, because the balance constraint (Eq. 5.4) ensures that edges are uniformly distributed over machines, we naturally achieve improved work balance even in the presence of very high-degree vertices.

The simplest method to construct a vertex cut is to randomly assign edges to machines. Random (hashed) edge placement is fully data-parallel, achieves nearly perfect balance on large graphs, and can be applied in the streaming setting. In the following theorem, we relate the expected normalized replication factor (Eq. 5.3) to the number of machines and the power-law constant α .

Theorem 5.2 (Randomized Vertex Cuts). *A random vertex-cut on p machines has an expected replication:*

$$\mathbb{E} \left[\frac{1}{|V|} \sum_{v \in V} |A(v)| \right] = \frac{p}{|V|} \sum_{v \in V} \left(1 - \left(1 - \frac{1}{p} \right)^{\mathbf{D}[v]} \right). \quad (5.5)$$

where $\mathbf{D}[v]$ denotes the degree of vertex v . For a power-law graph the expected replication (Fig. 6a) is determined entirely by the power-law constant α :

$$\mathbb{E} \left[\frac{1}{|V|} \sum_{v \in V} |A(v)| \right] = p - \frac{p}{\mathbf{h}_{|V|}(\alpha)} \sum_{d=1}^{|V|-1} \left(\frac{p-1}{p} \right)^d d^{-\alpha}, \quad (5.6)$$

where $\mathbf{h}_{|V|}(\alpha) = \sum_{d=1}^{|V|-1} d^{-\alpha}$ is the normalizing constant of the power-law Zipf distribution.

Proof. By linearity of expectation:

$$\mathbb{E} \left[\frac{1}{|V|} \sum_{v \in V} |A(v)| \right] = \frac{1}{|V|} \sum_{v \in V} \mathbb{E}[|A(v)|], \quad (5.7)$$

The expected replication $\mathbb{E}[|A(v)|]$ of a single vertex v can be computed by considering the process of randomly assigning the $\mathbf{D}[v]$ edges adjacent to v . Let the indicator X_i denote the event that vertex v has at least one of its edges on machine i . The expectation $\mathbb{E}[X_i]$ is then:

$$\mathbb{E}[X_i] = 1 - \mathbf{P}(v \text{ has no edges on machine } i) \quad (5.8)$$

$$= 1 - \left(1 - \frac{1}{p} \right)^{\mathbf{D}[v]}, \quad (5.9)$$

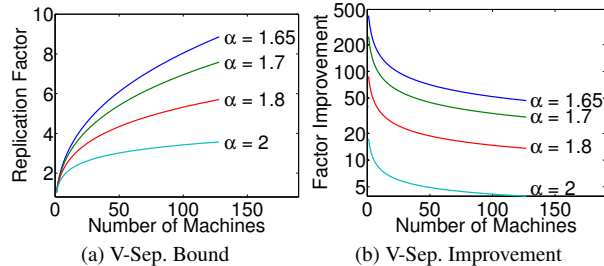


Figure 6: (a) Expected replication factor for different power-law constants. (b) The ratio of the expected communication and storage cost of random edge cuts to random vertex cuts as a function of the number machines. This graph assumes that edge data and vertex data are the same size.

The expected replication factor for vertex v is then:

$$\mathbb{E}[|A(v)|] = \sum_{i=1}^p \mathbb{E}[X_i] = p \left(1 - \left(1 - \frac{1}{p} \right)^{\mathbf{D}[v]} \right). \quad (5.10)$$

Treating $\mathbf{D}[v]$ as a Zipf random variable:

$$\mathbb{E} \left[\frac{1}{|V|} \sum_{v \in V} |A(v)| \right] = \frac{p}{|V|} \sum_{v \in V} \left(1 - \mathbb{E} \left[\left(\frac{p-1}{p} \right)^{\mathbf{D}[v]} \right] \right), \quad (5.11)$$

and taking the expectation under $\mathbf{P}(d) = d^{-\alpha} / \mathbf{h}_{|V|}(\alpha)$:

$$\mathbb{E} \left[\left(1 - \frac{1}{p} \right)^{\mathbf{D}[v]} \right] = \frac{1}{\mathbf{h}_{|V|}(\alpha)} \sum_{d=1}^{|V|-1} \left(1 - \frac{1}{p} \right)^d d^{-\alpha}. \quad (5.12)$$

While lower α values (more high-degree vertices) imply a higher replication factor (Fig. 6a) the effective gains of vertex-cuts relative to edge cuts (Fig. 6b) actually *increase* with lower α . In Fig. 6b we plot the ratio of the expected costs (comm. and storage) of random edge-cuts (Eq. 5.2) to the expected costs of random vertex-cuts (Eq. 5.6) demonstrating order of magnitude gains.

Finally, the vertex cut model is also highly effective for regular graphs since in the event that a good edge-cut can be found it can be converted to a better vertex cut:

Theorem 5.3. *For a given an edge-cut with g ghosts, any vertex cut along the same partition boundary has strictly fewer than g mirrors.*

Proof of Theorem 5.3. Consider the two-way edge cut which cuts the set of edges $E' \in E$ and let V' be the set of vertices in E' . The total number of ghosts induced by this edge partition is therefore $|V'|$. If we then select and delete arbitrary vertices from V' along with their adjacent edges until no edges remain, then the set of deleted vertices corresponds to a vertex-cut in the original graph. Since at most $|V'| - 1$ vertices may be deleted, there can be at most $|V'| - 1$ mirrors. \square

Graph	$ V $	$ E $	α	# Edges
Twitter [24]	41M	1.4B	1.8	641,383,778
UK [7]	132.8M	5.5B	1.9	245,040,680
Amazon [6, 5]	0.7M	5.2M	2.0	102,838,432
LiveJournal [12]	5.4M	79M	2.1	57,134,471
Hollywood [6, 5]	2.2M	229M	2.2	35,001,696

(a) Real world graphs

(b) Synthetic Graphs

Table 1: (a) A collection of Real world graphs. (b) Randomly constructed ten-million vertex power-law graphs with varying α . Smaller α produces denser graphs.

5.2 Greedy Vertex-Cuts

We can improve upon the randomly constructed vertex-cut by de-randomizing the edge-placement process. The resulting algorithm is a sequential greedy heuristic which places the next edge on the machine that minimizes the conditional expected replication factor. To construct the de-randomization we consider the task of placing the $i + 1$ edge after having placed the previous i edges. Using the conditional expectation we define the objective:

$$\arg \min_k \mathbb{E} \left[\sum_{v \in V} |A(v)| \mid A_i, A(e_{i+1}) = k \right], \quad (5.13)$$

where A_i is the assignment for the previous i edges. Using Theorem 5.2 to evaluate Eq. 5.13 we obtain the following edge placement rules for the edge (u, v) :

- Case 1:** If $A(u)$ and $A(v)$ intersect, then the edge should be assigned to a machine in the intersection.
- Case 2:** If $A(u)$ and $A(v)$ are not empty and do not intersect, then the edge should be assigned to one of the machines from the vertex with the most unassigned edges.
- Case 3:** If only one of the two vertices has been assigned, then choose a machine from the assigned vertex.
- Case 4:** If neither vertex has been assigned, then assign the edge to the least loaded machine.

Because the greedy-heuristic is a de-randomization it is guaranteed to obtain an expected replication factor that is no worse than random placement and in practice can be much better. Unlike the randomized algorithm, which is embarrassingly parallel and easily distributed, the greedy algorithm requires coordination between machines. We consider two distributed implementations:

Coordinated: maintains the values of $A_i(v)$ in a distributed table. Then each machine runs the greedy heuristic and periodically updates the distributed table. Local caching is used to reduce communication at the expense of accuracy in the estimate of $A_i(v)$.

Oblivious: runs the greedy heuristic independently on each machine. Each machine maintains its own estimate of A_i with no additional communication.

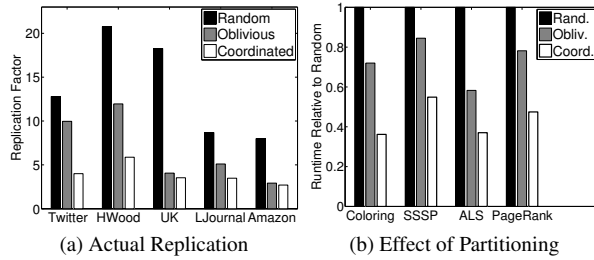


Figure 7: (a) The actual replication factor on 32 machines. (b) The effect of partitioning on runtime.

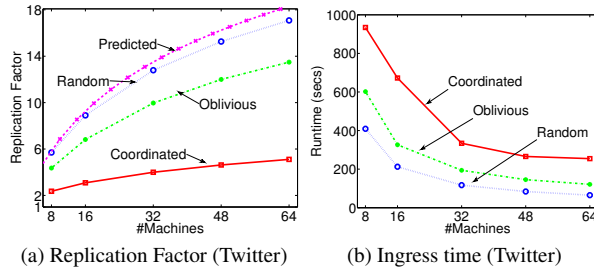


Figure 8: (a,b) Replication factor and runtime of graph ingress for the Twitter follower network as a function of the number of machines for random, oblivious, and coordinated vertex-cuts.

In Fig. 8a, we compare the replication factor of both heuristics against random vertex cuts on the Twitter follower network. We plot the replication factor as a function of the number of machines (EC2 instances described in Sec. 7) and find that random vertex cuts match the predicted replication given in Theorem 5.2. Furthermore, the greedy heuristics substantially improve upon random placement with an order of magnitude reduction in the replication factor, and therefore communication and storage costs. For a fixed number of machines ($p = 32$), we evaluated (Fig. 7a) the replication factor of the two heuristics on five real-world graphs (Tab. 1a). In all cases the greedy heuristics out-perform random placement, while doubling the load time (Fig. 8b). The Oblivious heuristic achieves compromise by obtaining a relatively low replication factor while only slightly increasing runtime.

6 Abstraction Comparison

In this section, we experimentally characterize the dependence on α and the relationship between fan-in and fan-out by using the Pregel, GraphLab, and PowerGraph abstractions to run PageRank on five synthetically constructed power-law graphs. Each graph has ten-million vertices and an α ranging from 1.8 to 2.2. The graphs were constructed by randomly sampling the out-degree of each vertex from a Zipf distribution and then adding out-edges such that the in-degree of each vertex is nearly identical. We then inverted each graph to obtain the corresponding power-law fan-in graph. The density of each power-law graph is determined by α and therefore each

graph has a different number of edges (see Tab. 1b).

We used the GraphLab v1 C++ implementation from [29] and added instrumentation to track network usage. As of the writing of this paper, public implementations of Pregel (e.g., Giraph) were unable to handle even our smaller synthetic problems due to memory limitations. Consequently, we used Piccolo [32] as a proxy implementation of Pregel since Piccolo naturally expresses the Pregel abstraction and provides an efficient C++ implementation with dynamic load-balancing. Finally, we used our implementation of PowerGraph described in Sec. 7.

All experiments in this section are evaluated on an eight node Linux cluster. Each node consists of two quad-core Intel Xeon E5620 processors with 32 GB of RAM and is connected via 1-GigE Ethernet. All systems were compiled with GCC 4.4. GraphLab and Piccolo used random edge-cuts while PowerGraph used random vertex-cuts. Results are averaged over 20 iterations.

6.1 Computation Imbalance

The *sequential* component of the PageRank vertex-program is proportional to out-degree in the Pregel abstraction and in-degree in the GraphLab abstraction. Alternatively, PowerGraph eliminates this sequential dependence by distributing the computation of *individual* vertex-programs over multiple machines. Therefore we expect, highly-skewed (low α) power-law graphs to increase work imbalance under the Pregel (fan-in) and GraphLab (fan-out) abstractions but not under the PowerGraph abstraction, which evenly distributed high-degree vertex-programs. To evaluate this hypothesis we ran eight “workers” per system (64 total workers) and recorded the vertex-program time on each worker.

In Fig. 9a and Fig. 9b we plot the *standard deviation* of worker per-iteration runtimes, a measure of work imbalance, for power-law fan-in and fan-out graphs respectively. Higher standard deviation implies greater imbalance. While lower α increases work imbalance for GraphLab (on fan-in) and Pregel (on fan-out), the PowerGraph abstraction is unaffected in either edge direction.

6.2 Communication Imbalance

Because GraphLab and Pregel use edge-cuts, their communication volume is proportional to the number of ghosts: the replicated vertex and edge data along the partition boundary. If one message is sent per edge, Pregel’s combiners ensure that exactly one network message is transmitted for each ghost. Similarly, at the end of each iteration GraphLab synchronizes each ghost and thus the communication volume is also proportional to the number of ghosts. PowerGraph on the other hand uses vertex-cuts and only synchronizes mirrors after each iteration. The communication volume of a complete iteration is therefore proportional to the number of mirrors induced by the

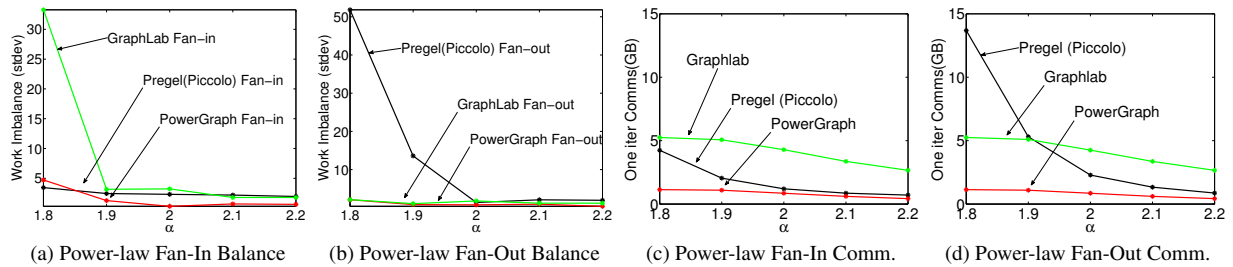


Figure 9: **Synthetic Experiments: Work Imbalance and Communication.** (a, b) Standard deviation of worker computation time across 8 distributed workers for each abstraction on power-law fan-in and fan-out graphs. (b, c) Bytes communicated per iteration for each abstraction on power-law fan-in and fan-out graphs.

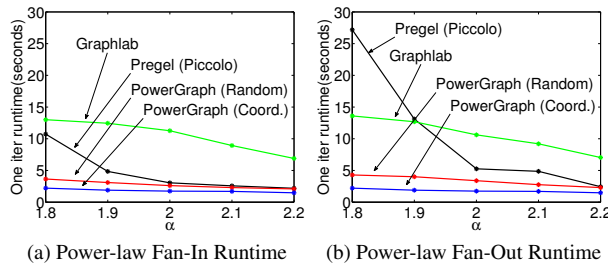


Figure 10: **Synthetic Experiments Runtime.** (a, b) Per iteration runtime of each abstraction on synthetic power-law graphs.

vertex-cut. As a consequence we expect that PowerGraph will reduce communication volume.

In Fig. 9c and Fig. 9d we plot the bytes communicated per iteration for all three systems under power-law fan-in and fan-out graphs. Because Pregel only sends messages along out-edges, Pregel communicates more on power-law fan-out graphs than on power-law fan-in graphs.

On the other hand, GraphLab and PowerGraph’s communication volume is invariant to power-law fan-in and fan-out since neither considers edge direction during data-synchronization. However, PowerGraph communicates significantly less than GraphLab which is a direct result of the efficacy of vertex cuts. Finally, PowerGraph’s total communication increases only marginally on the denser graphs and is the lowest overall.

6.3 Runtime Comparison

PowerGraph significantly out-performs GraphLab and Pregel on low α graphs. In Fig. 10a and Fig. 10b we plot the per iteration runtime for each abstraction. In both cases the overall runtime performance closely matches the communication overhead (Fig. 9c and Fig. 9d) while the computation imbalance (Fig. 9a and Fig. 9b) appears to have little effect. The limited effect of imbalance is due to the relatively lightweight nature of the PageRank computation and we expect more complex algorithms (e.g., statistical inference) to be more susceptible to imbalance. However, when greedy (coordinated) partitioning is used we see an additional 25% to 50% improvement in runtime.

7 Implementation and Evaluation

In this section, we describe and evaluate our implementation of the PowerGraph system. All experiments are performed on a 64 node cluster of Amazon EC2 `cc1.4xlarge` Linux instances. Each instance has two quad core Intel Xeon X5570 processors with 23GB of RAM, and is connected via 10 GigE Ethernet. PowerGraph was written in C++ and compiled with GCC 4.5.

We implemented three variations of the PowerGraph abstraction. To demonstrate their relative implementation complexity, we provide the line counts, excluding common support code:

Bulk Synchronous (Sync): A fully synchronous implementation of PowerGraph as described in Sec. 4.3.1. [600 lines]

Asynchronous (Async): An asynchronous implementation of PowerGraph which allows arbitrary interleaving of vertex-programs Sec. 4.3.2. [900 lines]

Asynchronous Serializable (Async+S): An asynchronous implementation of PowerGraph which guarantees serializability of *all* vertex-programs (equivalent to “edge consistency” in GraphLab). [1600 lines]

In all cases the system is entirely symmetric with no single coordinating instance or scheduler. Each instances is given the list of other machines and start by reading a unique subset of the graph data files from HDFS. TCP connections are opened with other machines as needed to build the distributed graph and run the engine.

7.1 Graph Loading and Placement

The graph structure and data are loaded from a collection of text files stored in a distributed file-system (HDFS) by all instances in parallel. Each machine loads a separate subset of files (determined by hashing) and applies one of the three distributed graph partitioning algorithms to place the data *as it is loaded*. As a consequence partitioning is accomplished in parallel and data is immediately placed in its final location. Unless specified, all experiments were performed using the oblivious algorithm. Once computation is complete, the final vertex and edge data are saved back to the distributed file-system in parallel.

In Fig. 7b, we evaluate the performance of a collection of algorithms varying the partitioning procedure. Our simple partitioning heuristics are able to improve performance significantly across *all algorithms*, decreasing runtime and memory utilization. Furthermore, the runtime scales *linearly* with the replication factor: halving the replication factor approximately halves runtime.

7.2 Synchronous Engine (Sync)

Our synchronous implementation closely follows the description in Sec. 4.3.1. Each machine runs a single multi-threaded instance to maximally utilize the multi-core architecture. We rely on background communication to achieve computation/communication interleaving. The synchronous engine’s fully deterministic execution makes it easy to reason about programmatically and minimizes effort needed for tuning and performance optimizations.

In Fig. 11a and Fig. 11b we plot the runtime and total communication of one iteration of PageRank on the Twitter follower network for each partitioning method. To provide a point of comparison (Tab. 2), the Spark [37] framework computes one iteration of PageRank on the same graph in 97.4s on a 50 node-100 core cluster [35]. PowerGraph is therefore between 3-8x faster than Spark on a comparable number of cores. On the full cluster of 512 cores, we can compute one iteration in 3.6s.

The greedy partitioning heuristics improves both performance and scalability of the engine at the cost of increased load-time. The load time for random, oblivious, and coordinated placement were 59, 105, and 239 seconds respectively. While greedy partitioning heuristics increased load-time by up to a factor of four, they still improve overall runtime if more than 20 iterations of PageRank are performed. In Fig. 11c we plot the runtime of each iteration of PageRank on the Twitter follower network. Delta caching improves performance by avoiding unnecessary gather computation, decreasing total runtime by 45%. Finally, in Fig. 11d we evaluate weak-scaling: ability to scale while keeping the problem size per processor constant. We run SSSP (Fig. 3) on synthetic power-law graphs ($\alpha = 2$), with ten-million vertices per machine. Our implementation demonstrates nearly optimal weak-scaling and requires only 65s to solve a 6.4B edge graph.

7.3 Asynchronous Engine (Async)

We implemented the asynchronous PowerGraph execution model (Sec. 4.3.2) using a simple state machine for each vertex which can be either: `INACTIVE`, `GATHER`, `APPLY` or `SCATTER`. Once activated, a vertex enters the gathering state and is placed in a *local* scheduler which assigns cores to active vertices allowing many vertex-programs to run simultaneously thereby hiding communication latency. While arbitrary interleaving of vertex

programs is permitted, we avoid data races by ensuring that individual gather, apply, and scatter calls have exclusive access to their arguments.

We evaluate the performance of the Async engine by running PageRank on the Twitter follower network. In Fig. 12a, we plot throughput (number of vertex-program operations per second) against the number of machines. Throughput increases moderately with both the number of machines as well as improved partitioning. We evaluate the gains associated with delta caching (Sec. 4.2) by measuring throughput as a function of time (Fig. 12b) with caching enabled and with caching disabled. Caching allows the algorithm to converge faster with fewer operations. Surprisingly, when caching is disabled, the throughput increases over time. Further analysis reveals that the computation gradually focuses on high-degree vertices, increasing the computation/communication ratio.

We evaluate the graph coloring vertex-program (Fig. 3) which cannot be run synchronously since all vertices would change to the same color on every iteration. Graph coloring is a proxy for many MLDM algorithms [17]. In Fig. 12c we evaluate weak-scaling on synthetic power-law graphs ($\alpha = 2$) with five-million vertices per machine and find that the Async engine performs nearly optimally. The slight increase in runtime may be attributed to an increase in the number of colors due to increasing graph size.

7.4 Async. Serializable Engine (Async+S)

The Async engine is useful for a broad range of tasks, providing high throughput and performance. However, unlike the synchronous engine, the asynchronous engine is difficult to reason about programmatically. We therefore extended the Async engine to enforce serializability.

The Async+S engine ensures serializability by preventing adjacent vertex-programs from running simultaneously. Ensuring serializability for graph-parallel computation is equivalent to solving the dining philosophers problem where each vertex is a philosopher, and each edge is a fork. GraphLab [29] implements Dijkstra’s solution [14] where forks are acquired *sequentially* according to a total ordering. Instead, we implement the Chandy-Misra solution [10] which acquires all forks simultaneously, permitting a high degree of parallelism. We extend the Chandy-Misra solution to the vertex-cut setting by enabling each vertex replica to request only forks for local edges and using a simple consensus protocol to establish when all replicas have succeeded.

We evaluate the scalability and computational efficiency of the Async+S engine on the graph coloring task. We observe in Fig. 12c that the amount of achieved parallelism does not increase linearly with the number of vertices. Because the density (i.e., contention) of power-law graphs increases super-linearly with the number of

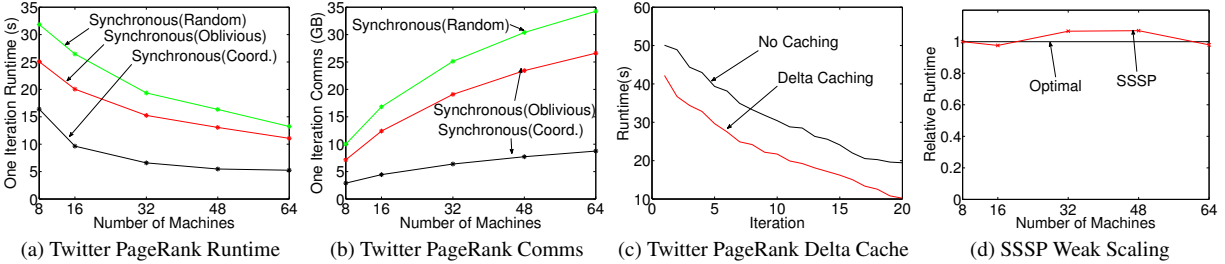


Figure 11: **Synchronous Experiments (a,b)** Synchronous PageRank Scaling on Twitter graph. **(c)** The PageRank per iteration runtime on the Twitter graph with and without delta caching. **(d)** Weak scaling of SSSP on synthetic graphs.

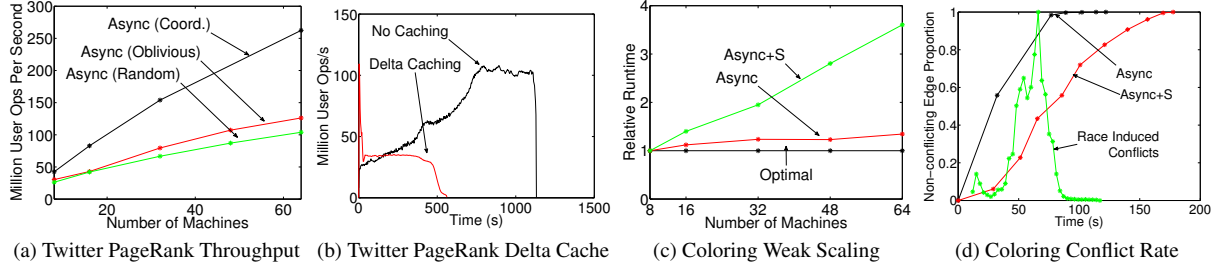


Figure 12: **Asynchronous Experiments (a)** Number of user operations (gather/apply/scatter) issued per second by Dynamic PageRank as # machines is increased. **(b)** Total number of user ops with and without caching plotted against time. **(c)** Weak scaling of the graph coloring task using the Async engine and the Async+S engine **(d)** Proportion of non-conflicting edges across time on a 8 machine, 40M vertex instance of the problem. The green line is the rate of conflicting edges introduced by the lack of consistency (peak 236K edges per second) in the Async engine. When the Async+S engine is used no conflicting edges are ever introduced.

vertices, we do not expect the amount of serializable parallelism to increase linearly.

In Fig. 12d, we plot the proportion of edges that satisfy the coloring condition (both vertices have different colors) for both the Async and the Async+S engines. While the Async engine quickly satisfies the coloring condition for most edges, the remaining 1% take 34% of the runtime. We attribute this behavior to frequent races on tightly connected vertices. Alternatively, the Async+S engine performs more uniformly. If we examine the total number of user operations we find that the Async engine does more than *twice* the work of the Async+S engine.

Finally, we evaluate the Async and the Async+S engines on a popular machine learning algorithm: Alternating Least Squares (ALS). The ALS algorithm has a number of variations which allow it to be used in a wide range of applications including user personalization [38] and document semantic analysis [21]. We apply ALS to the Wikipedia term-document graph consisting of 11M vertices and 315M edges to extract a mixture of topics representation for each document and term. The number of topics d is a free parameter that determines the computational complexity $O(d^3)$ of each vertex-program. In Fig. 13a, we plot the ALS throughput on the Async engine and the Async+S engine. While the throughput of the Async engine is greater, the gap between engines shrinks as d increases and computation dominates the consistency overhead. To demonstrate the importance of serializabil-

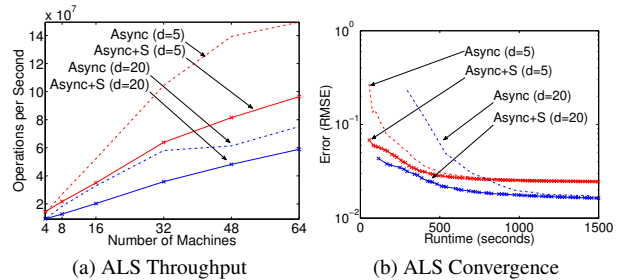


Figure 13: **(a)** The throughput of ALS measured in millions of User Operations per second. **(b)** Training error (lower is better) as a function of running time for ALS application.

ity, we plot in Fig. 13b the training error, a measure of solution quality, for both engines. We observe that while the Async engine has greater throughput, the Async+S engine *converges* faster.

The complexity of the Async+S engine is justified by the necessity for serializability in many applications (e.g., ALS). Furthermore, serializability adds predictability to the nondeterministic asynchronous execution. For example, even graph coloring may not terminate on dense graphs unless serializability is ensured.

7.5 Fault Tolerance

Like GraphLab and Pregel, PowerGraph achieves fault-tolerance by saving a snapshot of the data-graph. The synchronous PowerGraph engine constructs the snapshot between super-steps and the asynchronous engine suspends

PageRank	Runtime	V	E	System
Hadoop [22]	198s	–	1.1B	50x8
Spark [37]	97.4s	40M	1.5B	50x2
Twister [15]	36s	50M	1.4B	64x4
<i>PowerGraph (Sync)</i>	3.6s	40M	1.5B	64x8

Triangle Count	Runtime	V	E	System
Hadoop [36]	423m	40M	1.4B	1636x?
<i>PowerGraph (Sync)</i>	1.5m	40M	1.4B	64x16

LDA	Tok/sec	Topics	System
<i>Smola et al.</i> [34]	150M	1000	100x8
<i>PowerGraph (Async)</i>	110M	1000	64x16

Table 2: Relative performance of PageRank, triangle counting, and LDA on similar graphs. PageRank runtime is measured per iteration. Both PageRank and triangle counting were run on the Twitter follower network and LDA was run on Wikipedia. The systems are reported as number of nodes by number of cores.

execution to construct the snapshot. An asynchronous snapshot using GraphLab’s snapshot algorithm [29] can also be implemented. The checkpoint overhead, typically a few seconds for the largest graphs we considered, is small relative to the running time of each application.

7.6 MLDM Applications

In Tab. 2 we provide comparisons of the PowerGraph system with published results on similar data for PageRank, Triangle Counting [36], and collapsed Gibbs sampling for the LDA model [34]. The PowerGraph implementations of PageRank and Triangle counting are one to two orders of magnitude faster than published results. For LDA, the state-of-the-art solution is a heavily optimized system designed for this specific task by Smola et al. [34]. In contrast, PowerGraph is able to achieve comparable performance using only 200 lines of user code.

8 Related Work

The vertex-cut approach to distributed graph placement is related to work [9, 13] in hypergraph partitioning. In particular, a vertex-cut problem can be cast as a hypergraph-cut problem by converting each edge to a vertex, and each vertex to a hyper-edge. However, existing hypergraph partitioning can be very time intensive. While our cut objective is similar to the “communication volume” objective, the streaming vertex cut setting described in this paper is novel. Stanton et al, in [35] developed several heuristics for the streaming edge-cuts but do not consider the vertex-cut problem.

Several [8, 22] have proposed generalized sparse matrix vector multiplication as a basis for graph-parallel computation. These abstractions operate on commutative associative semi-rings and therefore also have generalized gather and sum operations. However, they do not support

the more general apply and scatter operations, as well as mutable edge-data and are based on a strictly synchronous model in which all computation is run in every iteration.

While we discuss Pregel and GraphLab in detail, there are other similar graph-parallel abstractions. Closely related to Pregel is BPGL [20] which implements a synchronous traveler model. Alternatively, Kineograph [11] presents a graph-parallel framework for time-evolving graphs which mixes features from both GraphLab and Piccolo. Pujol et al. [33] present a distributed graph database but do not explicitly consider the power-law structure. Finally, [25] presents GraphChi: an efficient single-machine disk-based implementation of the GraphLab abstraction. Impressively, it is able to significantly out-perform large Hadoop deployments on many graph problems while using only a single machine: performing one iteration of PageRank on the Twitter Graph in only 158s (PowerGraph: 3.6s). The techniques described in GraphChi can be used to add out-of-core storage to PowerGraph.

9 Conclusions and Future Work

The need to reason about large-scale graph-structured data has driven the development of new graph-parallel abstractions such as GraphLab and Pregel. However graphs derived from real-world phenomena often exhibit power-law degree distributions, which are difficult to partition and can lead to work imbalance and substantially increased communication and storage.

To address these challenges, we introduced the PowerGraph abstraction which exploits the Gather-Apply-Scatter model of computation to factor vertex-programs over edges, splitting high-degree vertices and exposing greater parallelism in natural graphs. We then introduced vertex-cuts and a collection of fast greedy heuristics to substantially reduce the storage and communication costs of large distributed power-law graphs. We theoretically related the power-law constant to the communication and storage requirements of the PowerGraph system and empirically evaluate our analysis by comparing against GraphLab and Pregel. Finally, we evaluate the PowerGraph system on several large-scale problems using a 64 node EC2 cluster and demonstrating the scalability and efficiency and in many cases order of magnitude gains over published results.

We are actively using PowerGraph to explore new large-scale machine learning algorithms. We are beginning to study how vertex replication and data-dependencies can be used to support fault-tolerance without checkpointing. In addition, we are exploring ways to support time-evolving graph structures. Finally, we believe that many of the core ideas in the PowerGraph abstraction can have a significant impact in the design and implementation of graph-parallel systems beyond PowerGraph.

Acknowledgments

This work is supported by the ONR Young Investigator Program grant N00014-08-1-0752, the ARO under MURI W911NF0810242, the ONR PECASE-N00014-10-1-0672, the National Science Foundation grant IIS-0803333 as well as the Intel Science and Technology Center for Cloud Computing. Joseph Gonzalez is supported by the Graduate Research Fellowship from the NSF. We would like to thank Alex Smola, Aapo Kyrola, Lidong Zhou, and the reviewers for their insightful guidance.

References

- [1] ABOU-RJEILI, A., AND KARYPIS, G. Multilevel algorithms for partitioning power-law graphs. In *IPDPS* (2006).
- [2] AHMED, A., ALY, M., GONZALEZ, J., NARAYANAMURTHY, S., AND SMOLA, A. J. Scalable inference in latent variable models. In *WSDM* (2012), pp. 123–132.
- [3] ALBERT, R., JEONG, H., AND BARABÁSI, A. L. Error and attack tolerance of complex networks. In *Nature* (2000), vol. 406, pp. 378–482.
- [4] BERTSEKAS, D. P., AND TSITSIKLIS, J. N. *Parallel and distributed computation: numerical methods*. Prentice-Hall, 1989.
- [5] BOLDI, P., ROSA, M., SANTINI, M., AND VIGNA, S. Layered label propagation: A multiresolution coordinate-free ordering for compressing social networks. In *WWW* (2011), pp. 587–596.
- [6] BOLDI, P., AND VIGNA, S. The WebGraph framework I: Compression techniques. In *WWW* (2004), pp. 595–601.
- [7] BORDINO, I., BOLDI, P., DONATO, D., SANTINI, M., AND VIGNA, S. Temporal evolution of the uk web. In *ICDM Workshops* (2008), pp. 909–918.
- [8] BULUÇ, A., AND GILBERT, J. R. The combinatorial bias: design, implementation, and applications. *IJHPCA* 25, 4 (2011), 496–509.
- [9] CATALYUREK, U., AND AYKANAT, C. Decomposing irregularly sparse matrices for parallel matrix-vector multiplication. In *IRREGULAR* (1996), pp. 75–86.
- [10] CHANDY, K. M., AND MISRA, J. The drinking philosophers problem. *ACM Trans. Program. Lang. Syst.* 6, 4 (Oct. 1984), 632–646.
- [11] CHENG, R., HONG, J., KYROLA, A., MIAO, Y., WENG, X., WU, M., YANG, F., ZHOU, L., ZHAO, F., AND CHEN, E. Kineograph: taking the pulse of a fast-changing and connected world. In *EuroSys* (2012), pp. 85–98.
- [12] CHIERICHETTI, F., KUMAR, R., LATTANZI, S., MITZENMACHER, M., PANCONESI, A., AND RAGHAVAN, P. On compressing social networks. In *KDD* (2009), pp. 219–228.
- [13] DEVINE, K. D., BOMAN, E. G., HEAPHY, R. T., BISSELING, R. H., AND CATALYUREK, U. V. Parallel hypergraph partitioning for scientific computing. In *IPDPS* (2006).
- [14] DIJKSTRA, E. W. Hierarchical ordering of sequential processes. *Acta Informatica* 1 (1971), 115–138.
- [15] EKANAYAKE, J., LI, H., ZHANG, B., GUNARATHNE, T., BAE, S., QIU, J., AND FOX, G. Twister: A runtime for iterative MapReduce. In *HPDC* (2010), ACM.
- [16] FALOUTSOS, M., FALOUTSOS, P., AND FALOUTSOS, C. On power-law relationships of the internet topology. *ACM SIGCOMM Computer Communication Review* 29, 4 (1999), 251–262.
- [17] GONZALEZ, J., LOW, Y., GRETTON, A., AND GUESTRIN, C. Parallel gibbs sampling: From colored fields to thin junction trees. In *AISTATS* (2011), vol. 15, pp. 324–332.
- [18] GONZALEZ, J., LOW, Y., AND GUESTRIN, C. Residual splash for optimally parallelizing belief propagation. In *AISTATS* (2009), vol. 5, pp. 177–184.
- [19] GONZALEZ, J., LOW, Y., GUESTRIN, C., AND O’HALLARON, D. Distributed parallel inference on large factor graphs. In *UAI* (2009).
- [20] GREGOR, D., AND LUMSDAINE, A. The parallel BGL: A generic library for distributed graph computations. *POOSC* (2005).
- [21] HOFMANN, T. Probabilistic latent semantic indexing. In *SIGIR* (1999), pp. 50–57.
- [22] KANG, U., TSOURAKAKIS, C. E., AND FALOUTSOS, C. Pegasus: A peta-scale graph mining system implementation and observations. In *ICDM* (2009), pp. 229–238.
- [23] KARYPIS, G., AND KUMAR, V. Multilevel k-way partitioning scheme for irregular graphs. *J. Parallel Distrib. Comput.* 48, 1 (1998), 96–129.
- [24] KWAK, H., LEE, C., PARK, H., AND MOON, S. What is twitter, a social network or a news media? In *WWW* (2010), pp. 591–600.
- [25] KYROLA, A., BLELLOCH, G., AND GUESTRIN, C. GraphChi: Large-scale graph computation on just a PC. In *OSDI* (2012).
- [26] LANG, K. Finding good nearly balanced cuts in power law graphs. Tech. Rep. YRL-2004-036, Yahoo! Research Labs, Nov. 2004.
- [27] LESKOVEC, J., KLEINBERG, J., AND FALOUTSOS, C. Graph evolution: Densification and shrinking diameters. *ACM Trans. Knowl. Discov. Data* 1, 1 (mar 2007).
- [28] LESKOVEC, J., LANG, K. J., DASGUPTA, A., AND MAHONEY, M. W. Community structure in large networks: Natural cluster sizes and the absence of large well-defined clusters. *Internet Mathematics* 6, 1 (2008), 29–123.
- [29] LOW, Y., GONZALEZ, J., KYROLA, A., BICKSON, D., GUESTRIN, C., AND HELLERSTEIN, J. M. Distributed GraphLab: A Framework for Machine Learning and Data Mining in the Cloud. *PVLDB* (2012).
- [30] MALEWICZ, G., AUSTERN, M. H., BIK, A. J., DEHNERT, J., HORN, I., LEISER, N., AND CZAJKOWSKI, G. Pregel: a system for large-scale graph processing. In *SIGMOD* (2010).
- [31] PELLEGRINI, F., AND ROMAN, J. Scotch: A software package for static mapping by dual recursive bipartitioning of process and architecture graphs. In *HPCN Europe* (1996), pp. 493–498.
- [32] POWER, R., AND LI, J. Piccolo: building fast, distributed programs with partitioned tables. In *OSDI* (2010).
- [33] PUJOL, J. M., ERRAMILLI, V., SIGANOS, G., YANG, X., LAOUTARIS, N., CHHABRA, P., AND RODRIGUEZ, P. The little engine(s) that could: scaling online social networks. In *SIGCOMM* (2010), pp. 375–386.
- [34] SMOLA, A. J., AND NARAYANAMURTHY, S. An Architecture for Parallel Topic Models. *PVLDB* 3, 1 (2010), 703–710.
- [35] STANTON, I., AND KLIOT, G. Streaming graph partitioning for large distributed graphs. Tech. Rep. MSR-TR-2011-121, Microsoft Research, November 2011.
- [36] SURI, S., AND VASSILVITSKII, S. Counting triangles and the curse of the last reducer. In *WWW* (2011), pp. 607–614.
- [37] ZAHARIA, M., CHOWDHURY, M., FRANKLIN, M. J., SHENKER, S., AND STOICA, I. Spark: Cluster computing with working sets. In *HotCloud* (2010).
- [38] ZHOU, Y., WILKINSON, D., SCHREIBER, R., AND PAN, R. Large-scale parallel collaborative filtering for the netflix prize. In *AAIM* (2008), pp. 337–348.